

Thermal Ignition: Effects of Fuel, Ambient Pressure and Nitrogen Dilution

Conor D. Martin & Joseph E. Shepherd

Graduate Aerospace Laboratories, California Institute of Technology, Pasadena, CA, U.S.A

E-mail: cdmartin@caltech.edu

Abstract

We report new results for the pressure and nitrogen dilution dependence of thermal ignition thresholds of laminar external natural convection flows on a hot vertical cylinder. Experiments were conducted using an electrically-heated vertical cylinder (25.4 cm long, 2.54 cm diameter) in a 40 L vessel. Mixtures investigated included stoichiometric n-hexane, hydrogen and ethylene in oxygen/nitrogen atmospheres. A range of initial pressures (1, 0.7, 0.466, 0.238 atm) and nitrogen dilution levels ($N_2/O_2 = \beta = 3.76, 5.64, \text{ and } 7.52$, equivalent to $X_{O_2} = 20.6, 14.8, 11.6\%$) were explored for n-hexane. Two-color pyrometry was used to measure and control the cylinder surface temperature. Surface chemistry effects during hydrogen ignition testing provided further insight into the effectiveness of the two-color pyrometry measurement technique. Measurements of ignition threshold temperatures also have an intrinsic variability and were analyzed using a logistic regression methodology with the temperature corresponding to an ignition probability of 50% is reported as the ignition temperature. The ignition threshold for atmospheric hydrogen and ethylene were 982 ± 30 K and 996 ± 30 K respectively. These results are consistent with previous studies which have shown a positive correlation in ignition threshold and fuel molecular weight. A modest increase of ignition temperature threshold was observed for both decreasing pressure and increasing nitrogen concentration at fixed stoichiometry for hexane-air mixtures. A semi-empirical correlation based on the work of Ono et al. (1976) was found to be a reasonable representation of the pressure dependence for each β .

Keywords: *Thermal Ignition, Hydrogen, Hydrocarbon Fuel, Sub-atmospheric Pressure, Nitrogen Dilution*

1 Introduction

Accidental thermal ignition events are a significant potential hazard in many industrial applications including chemical processing, transportation and aviation. A thorough understanding of the conditions underlying these ignition processes is necessary to evaluate and mitigate potential hazards. Laboratory investigations of surface geometries and orientation have led to conflicting results, particularly for larger size surfaces that are encountered in industrial settings. For hot surface ignition, it is important to consider the fluid motion induced by buoyancy and a crucial distinction must be made between external and internal natural convection flows (Jones and Shepherd, 2021, Martin and Shepherd, 2021).

We have performed extensive testing in our laboratory with various fuels (See the discussion in Martin and Shepherd, 2021, Jones, 2020); in the present study we have focused on n-hexane, using this as a surrogate for aviation kerosene. Many other fuels are of interest in evaluating potential industrial hazards. For this study, we have also performed a limited number of ignition experiments with hydrogen and ethylene to enable comparisons with data from experiments with smaller heated surface area (Boeck et al., 2017) as well as the typical autoignition temperature

(AIT) criteria (ASTM, 2005).

Sub-atmospheric mixtures and mixtures with reduced oxygen concentration are of particular importance for aircraft fuel tank flammability reduction (FAA, 2017). Aircraft fuel tanks are vented to the atmosphere and pressures can be as low as 17 kPa (0.17 atm) at cruise altitudes of up to 13 km (43 kft). In order to minimize fuel tank flammability, nitrogen-enriching systems have been developed (Moravec et al., 2006), tested (Cavage and Summer, 2008) and are now extensively used in commercial aircraft. These systems are designed to reduce the oxygen concentration below the limiting value (approximately 12% by volume at ground level) for flammability. It is therefore of interest to understand how thermal ignition events are affected by variations in pressure and oxygen concentration. Summer (2004) used high-energy spark ignition and hot (≈ 1000 K) surfaces to establish limiting oxygen concentrations at sub-atmospheric pressures. However, the hot surface tests used a fixed geometry and surface temperature and did not quantify the thermal ignition threshold dependence on pressure and oxygen concentration.

The effect of pressure on thermal ignition thresholds has primarily been studied only at elevated pressures, for example Hirsch and Brandes (2005). Zabetakis (1965) report that flammability limits of alkane-air mixtures have a negligible dependence on pressure down to about 200 torr. Brandes et al. (2017a,b) studied ignition with elevated oxygen concentration (21-100%) and alternative oxidizers (N_2O) at atmospheric pressure. Those experiments involved internal natural convection (heated vessels) rather than external convection (heated surfaces). Ignition by external natural convection at reduced pressure was studied by Ono et al. (1976) who examined thermal ignition by small vertical hot plates ($1.5\text{-}9\text{ cm}^2$) at initial pressures between 0.13 and 1.0 atm. Ono et al. (1976) developed a semi empirical correlation between ignition temperature, surface height and pressure for laminar natural convection. With the exception of Summer (2004), two factor combinations of lowered pressure and oxygen content have not been systematically examined in previous studies.

The present study is an external natural convection experiment where the ignition source is a vertical cylinder. These experiments build upon the work performed by Jones and Shepherd (2021) who investigated thermal ignition by vertical cylinders and the effects of both length and surface area on ignition. Jones' study explored ignition source surface areas ranging from 25 to 200 cm^2 for stoichiometric n-hexane/air mixtures as well as Jet A samples and surrogates. Jones and Shepherd (2021) demonstrated that contrary to previous attempts at correlating thermal ignition thresholds with area, in external natural convection there is only a very modest decrease in the ignition threshold with increased surface area. Therefore, the present study used only the largest cylinder from Jones and Shepherd (2021), labelled 200A (length = 25.4 cm, diameter = 2.54 cm, surface area = 200 cm^2) using hydrogen/air, ethylene/air mixtures, and n-hexane-oxygen-nitrogen mixtures at reduced pressures.

2 Experimental Methodology

The experimental setup is identical to that described by Jones and Shepherd (2021) and in more detail by Jones (2020). The surface is a vertical cylinder constructed from stainless steel tubing and heated resistively using a Magna Power XR5-600 computer controlled power supply. The experiments are conducted inside a 40 L cylindrical combustion vessel with a 30.4 cm inner diameter and a height of 66.0 cm. The cylinder is held in place in the center of the combustion vessel with a copper support structure as shown in Figure 1. The support structure both mechanically stabilizes the heated surface and provides a path for electrical current to flow from. The cylinder temperature is monitored using a custom built two-color pyrometer as well as a K-type thermocouple welded to the center of the cylinder. The thermocouple is not present for all tests as prolonged exposure to

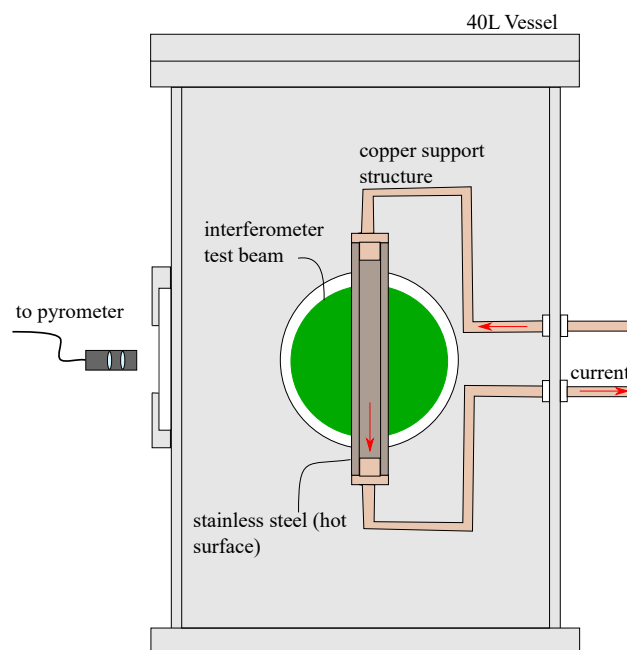


Fig. 1: Schematic of heated cylinder setup. (Adapted from Jones, 2020).

high temperatures tended to melt the spot weld and led the thermocouple to become disconnected from the surface periodically. For this reason, the pyrometer is found to be more reliable and is used in a feedback control loop with the power supply to maintain a set surface temperature. This system is controlled remotely via LabVIEW and the control loop is only initiated after an initial ramping period where the current supplied is fixed. The ends of the cylinder are water cooled using a NESLAB system III heat exchanger whose flow rate is adjusted using a ball valve and volumetric flow controller. This extracts the heat that otherwise would be conducted into the support structure during testing. A modified Mach-Zehnder interferometer in conjunction with a Phantom V7100 high speed camera is used to visualize ignition and make quantitative measurements of the gas surrounding the hot cylinder for nonreactive mixtures.

The method of partial pressures is used to control the gas conditions for each shot. The vessel is evacuated to less than 0.1 torr before the start of the filling process. The fuel is then added using either a syringe in the case of liquid fuels or a gas supply system for gaseous fuels. Nitrogen and oxygen are then added independently in appropriate amounts to make the desired fuel-air mixture. A capacitive pressure gauge (MKS model 121A-01000B) with an accuracy of 0.1 torr is used to monitor the pressure during filling. After the vessel is filled, a fan mixer is turned on for three minutes to promote mixing of the gases and then turned off for three minutes to allow the gases to settle and produce a quiescent mixture at the start of each test. The test time is limited to 300 s in order to prevent recirculation of the gas through the heated boundary layer. At the end of the test time if there has been no ignition, then the test is ended and is reported as a non-ignition result. In the cases where ignition occurred, the data acquisition system was triggered by a thermally-protected, piezoresistive pressure transducer (Endevco 8530B-200) which was used to record pressure rise during the test. The magnitude of the pressure rise and the appearance of a flame in the interferometer imaging were used to determine if ignition took place.

Ignition data were analyzed statistically by the logistic method, assigning to each shot a binary

outcome variable of 0 or 1, representing a non-ignition and ignition result respectively. Details of the logistic approach can be found in Bane et al. (2011), Jones (2020). Outcome data paired with the surface temperature (T_s) of each test demonstrate that there are both ignition and non-ignition cases at a given temperature near the ignition threshold. This overlap can be attributed to intrinsic uncertainty related to the ignition process as well as typical small experimental parameter (composition, temperature, heating ramp etc.) variability for tests nominally at the same initial conditions.

2.1 Surface Temperature Measurements

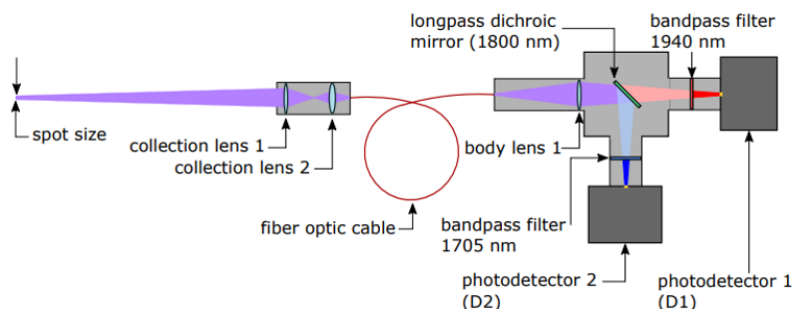


Fig. 2: Schematic of pyrometer construction with detectors, filters and collection optics shown (Adapted from Jones, 2020).

Non-contact measurements of surface temperature are made using a two-color pyrometer (Michalski and Michalski, 2001). The design is described in Jones (2020) and shown in Figure 2. The outputs of the detectors are analyzed using Planck’s law of blackbody radiation assuming gray-body (e.g. wavelength-independent) emissivity of the hot surface. The pyrometer was calibrated using a blackbody thermal radiation source (Process Sensors BBS1200) over a range of 700 – 1050°C in 25°C increments. Previous extensive testing (documented in Jones, 2020) using comparisons with thermocouple data indicates that this assumption is valid for oxidized, high temperature stainless steel surfaces. However, the surface conditions are a function of time and properties can significantly vary in some cases as discussed subsequently for hydrogen/air tests.

Pyrometry is an attractive technique for temperature measurement as this eliminates any flow disturbances introduced by spot welding a thermocouple wire to an otherwise uniformly smooth cylinder surface. A weld bead could potentially cause early onset of ignition by either forming a localized hot spot or by “tripping” the flow into the turbulent regime. We found that this was not a significant issue and to obtain reliable temperature measurements, we used both the thermocouple and the pyrometer during most ignition tests.

3 Results and discussion

A summary of all conditions studied are given in Table 1. Ignition thresholds for hydrogen and ethylene were obtained at only one condition, 1 atm and normal air composition and stoichiometric ratios of fuel to oxygen. Ignition thresholds for n-hexane were obtained for a range of initial pressures and nitrogen dilution levels. The initial pressures were chosen based on various altitudes in the standard atmosphere (e.g., $P_0 = 1, 0.7, 0.466,$ and 0.238 atm correspond to altitudes of 0, 10 kft, 20 kft, and 35 kft respectively). The hexane mixture compositions were defined by ϕC_6H_{14}

+ 9.5(O₂ + β N₂). Previous work on thermal ignition by Boeck et al. (2017) has shown minimal dependence of ignition threshold on equivalence ratio (ϕ) for n-hexane up to the flammability limits. This was confirmed in the present study by some preliminary testing on n-hexane mixtures ($\phi = 0.88, 1, 1.6, \beta = 3.76, P_0 = 1$ atm) with ignition temperature thresholds of 1020 K which are consistent with previous work by Jones (2020) and is well within the experimental uncertainty bounds of the pyrometer and logistic regression analysis. For all hexane tests, the composition used was stoichiometric.

Table 1: Summary of all experimental conditions and reported ignition temperatures (T_{ign}) with 95% confidence limits (95% CL) from logistic regression. Note that the uncertainty bounds on the pyrometer are much larger in all cases (± 30 K). All conditions are stoichiometric ($\phi=1.0$).

	β (X _{O₂} (%))	3.76 20.6	5.64 14.8	7.52 11.6	
Fuel	P_0 (atm)				
n-hexane	1.0	1020 ± 4	1045 ± 6	1066 ± 3	T_{ign} (K) 95% CL (K)
	0.7	1060 ± 5	1078 ± 5	1098 ± 3	T_{ign} (K) 95% CL (K)
	0.466	1091 ± 5	1119 ± 3	1128 ± 4	T_{ign} (K) 95% CL (K)
	0.238	1143 ± 4	1153 ± 5	1171 ± 1	T_{ign} (K) 95% CL (K)
hydrogen	1.0	982 ± 13	- -	- -	T_{ign} (K) 95% CL (K)
ethylene	1.0	996 ± 6	- -	- -	T_{ign} (K) 95% CL (K)

3.1 Hydrogen/Air

Hydrogen/air mixtures introduced some unexpected challenges that were not present in previous experiments working with n-hexane, Jet A or surrogate fuels. After several tests with hydrogen mixtures, we observed a large discrepancy in the temperatures recorded by the thermocouple and the pyrometer which had been in good agreement (± 10 K) in the hexane and ethylene tests. The reason became apparent upon visual inspection of the heated surface, see Figure 3. A reddish-orange oxide layer had formed on top of the gray-black oxide that normally persists on the surface. This layer is likely composed of Fe₃O₄ (gray) and Fe₂O₃ (red) or one of many possible hydrated iron oxides which will subsequently be referred to as "rust". No chemical analysis was conducted to confirm which oxides were present.

The "rust" build up could be sanded off along with the gray oxide layer, revealing the underlying polished steel surface. Before further testing using the pyrometer, the oxide layer then had to be rebuilt by holding the cylinder at an elevated temperature (1000 K) for 5-10 minutes in an air atmosphere. Once this was done the pyrometer readings again fell into agreement with the welded thermocouple (within ± 10 K). We therefore speculate that the differences in the wavelength dependence of the emissive properties of the rusty surface and the oxidized steel are the cause of this



Fig. 3: Comparison of the surface conditions observed in these experiments. (left) Polished stainless steel (middle) Typical oxide layer built up on surface after being held for 5-10 mins above 1000 K in an air atmosphere and (right) Surface after approximately 5 hydrogen ignition tests.

discrepancy. The rusted surface apparently is not a sufficiently gray body and there is substantial variation in the emissivity for the two wavelengths measured by the pyrometer.

The sensitivity of the surface temperature measurement to emissivity dependence on wavelength is substantial. For example a 3% difference in emissivity between the two wavelengths of interest will result in an approximately 40 K temperature difference. This is on the order of the discrepancy observed between the pyrometer and thermocouple measurements on the rusty surface. We found that the surface disruption and "rust" was found to develop for non-ignition cases as well as cases with ignition. This indicated that there was some significant reaction with hydrogen taking place near the surface in addition to the obvious potential of high temperature oxidation by water vapor in the post-combustion environment. This was also observable through a gradual decline in vessel pressure over the testing period. Similar declines were also evident in ignition cases in the lead up to ignition. This observation was in opposition to the pressure rise observed in tests with other fuels. A pressure rise is expected and was observed due to the bulk heating of the gas over the testing period of 300 s and slight decomposition of hydrocarbon species in the thermal boundary layer. However, decomposition of H_2 should lead to a decrease in total number of moles in the gas phase which would result in a declining pressure. The pressure data and surface change both indicate that there is significant low temperature decomposition in the case of hydrogen.

The procedure employed in performing the hydrogen tests therefore had to be modified to account for the heater surface changes. After each shot, the hot ignition products were immediately evacuated to minimize time exposed to the hot post-combustion products. Additionally, the surface was "cleaned" with sandpaper after every 5 shots and the gray oxidation layer was built back up before doing additional testing. Ignition kernels formed near the middle of the cylinder which was unique in that previously studied hydrocarbon fuels formed ignition kernels very close to the top of the heated surface (Jones, 2020). The results of the ignition testing were fit using a logistic regression and the results are shown in Figure 4. The ignition temperature was 982 ± 30 K. This corresponds to an ignition probability of 50% with the uncertainty determined by the pyrometer measurements.

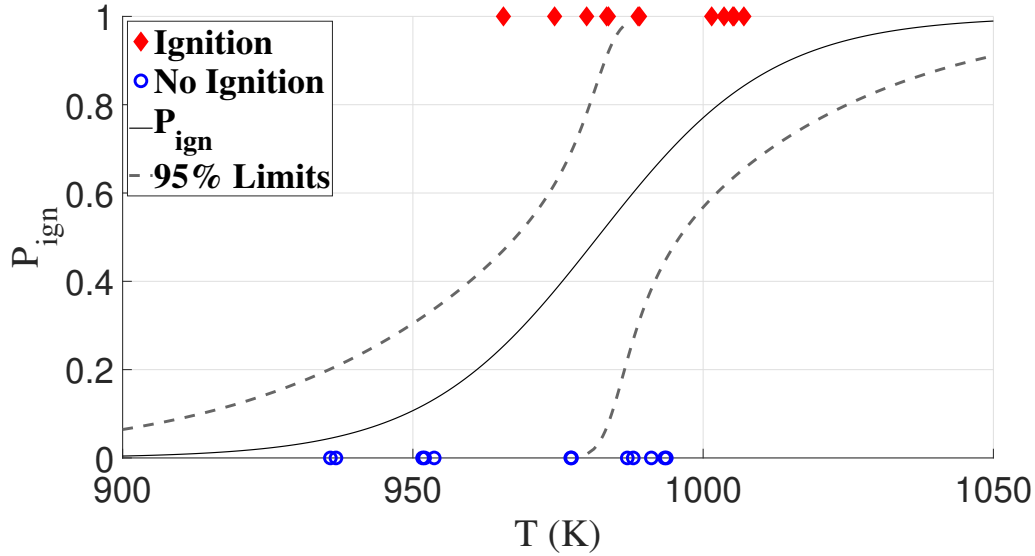


Fig. 4: Logistic regression of stoichiometric hydrogen/air ignition data.

3.2 Ethylene-Air

With the experience gained from the hydrogen tests, the ethylene/air shots were monitored closely for anomalous system behavior but none was observed. Ignition kernels formed near the top of the cylinder as was the case with other hydrocarbon fuels. Near the ignition threshold, ignition events appeared to be instigated by fluid ejections from the boundary layer. These ejections of hot fluid travel upward to the top of the cylinder where they are able to mix with hotter fluid at the top of the heated surface length where the thermal layer is thickest. It is unclear what role these ejections play in the early stages of ignition but they may contain some partially reacted mixture that would aid in instigating ignition and may promote mixing of fluid in the thermal layer. These ejections were also observed for n-hexane mixtures and nonreactive mixtures (pure nitrogen) so it seems they may be purely fluid mechanical in origin. The ignition data is presented in Fig. 5 and again fit with a logistic regression. The ignition temperature is $996 \pm 30\text{K}$ as determined by the 50% probability of ignition.

3.3 Sub-atmospheric n-hexane/oxygen/nitrogen mixtures

A two factor factorial experimental approach was taken to study 12 total test conditions consisting of mixtures of stoichiometric n-hexane/oxygen/nitrogen. The two factors under investigation were initial pressure and nitrogen dilution (equivalently, oxygen concentration). Each test condition was repeated at least 12 times to produce a statistically significant data set which could be reliably analyzed using the logistic regression approach. Full results are shown in Fig. 6 for all tests. These results demonstrate that decreasing pressure at fixed nitrogen dilution (constant β) results in increasing ignition temperatures. Similarly, increasing nitrogen dilution (β) at fixed initial pressure results in increasing ignition temperatures.

Figure 8 plots the ignition temperatures at fixed pressures against β . The ignition temperatures shown in this plot are those corresponding to 50% ignition probability as determined by the logistic curves shown in Fig. 6. The error bars correspond to the error in the pyrometer readings which

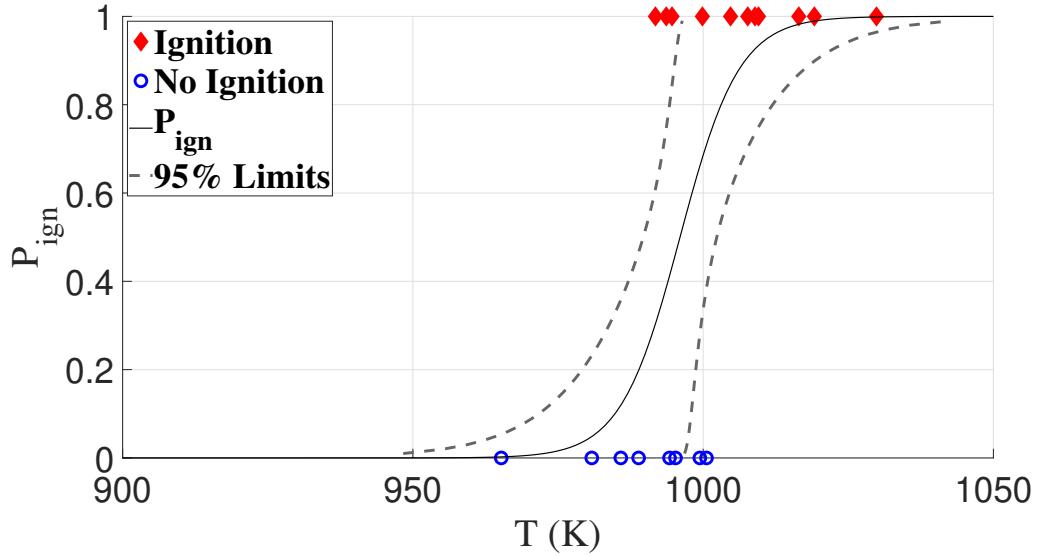


Fig. 5: Logistic regression of stoichiometric ethylene/air ignition data.

are estimated based on the 95% confidence intervals of the linear fit to the calibration data. This error is ± 30 K in this case which is much larger than the uncertainty resulting from the logistic regression to noisy ignition data which is only on the order of ± 3 -7 K in the cases shown in Fig. 6. Ignition temperatures for all pressures show a similar trend with β and vice versa. There does not appear to be any significant interaction between pressure and β effects on ignition thresholds in these experiments. Ignition was achieved for all pressures at 11.6% O_2 . This is in contrast to the results of Summer (2004) where limiting oxygen concentrations (LOC) of at least 14% were found for tests with a heated surface (~ 350 cm²) at temperatures up to about 1050 K using Jet fuels. The pressure for these tests was not stated. Summer's study primarily used a low-power arc of relatively short duration (1 s) and in those tests a LOC of around 12% was reported for sea level and increasing up to 14.5% for pressures corresponding to 40 kft altitude. Coward and Jones (1965) report a minimum LOC of 11.9% for n-hexane with nitrogen as the inerting agent. However this minimum was for slightly rich mixtures whereas for stoichiometric mixtures the LOC was 13.4%. The approach to determining flammability was the Explosion Tube Method and did not involve ignition by a hot surface but used an open flame. We did not dilute our mixtures systematically in order to determine the LOC but were able to obtain ignition at all pressures and dilution equivalent to an oxygen concentration of 11.6%.

Fig. 7 shows representative pressure traces obtained from an ignition experiment at each of the test conditions near the ignition thresholds. The plots show a reduction in peak pressure and decrease in the rate of pressure rise with increasing β . The decrease in the rate of pressure rise becomes especially evident at lower pressures. The decrease in peak pressure with increasing β and decreasing initial pressure is consistent with the thermodynamics of the combustion process. More dilute mixtures have lower energy content and consequently lower flame temperatures and peak adiabatic combustion pressures.

All other factors being the same, we expect that the peak pressure should scale directly with the initial pressure so that the ratio of peak pressure to initial pressure should depend mainly on β and have only a modest dependence on initial pressure. The decrease in pressure rise rate with increasing β is consistent with the decrease in observed and computed flame speeds for diluted

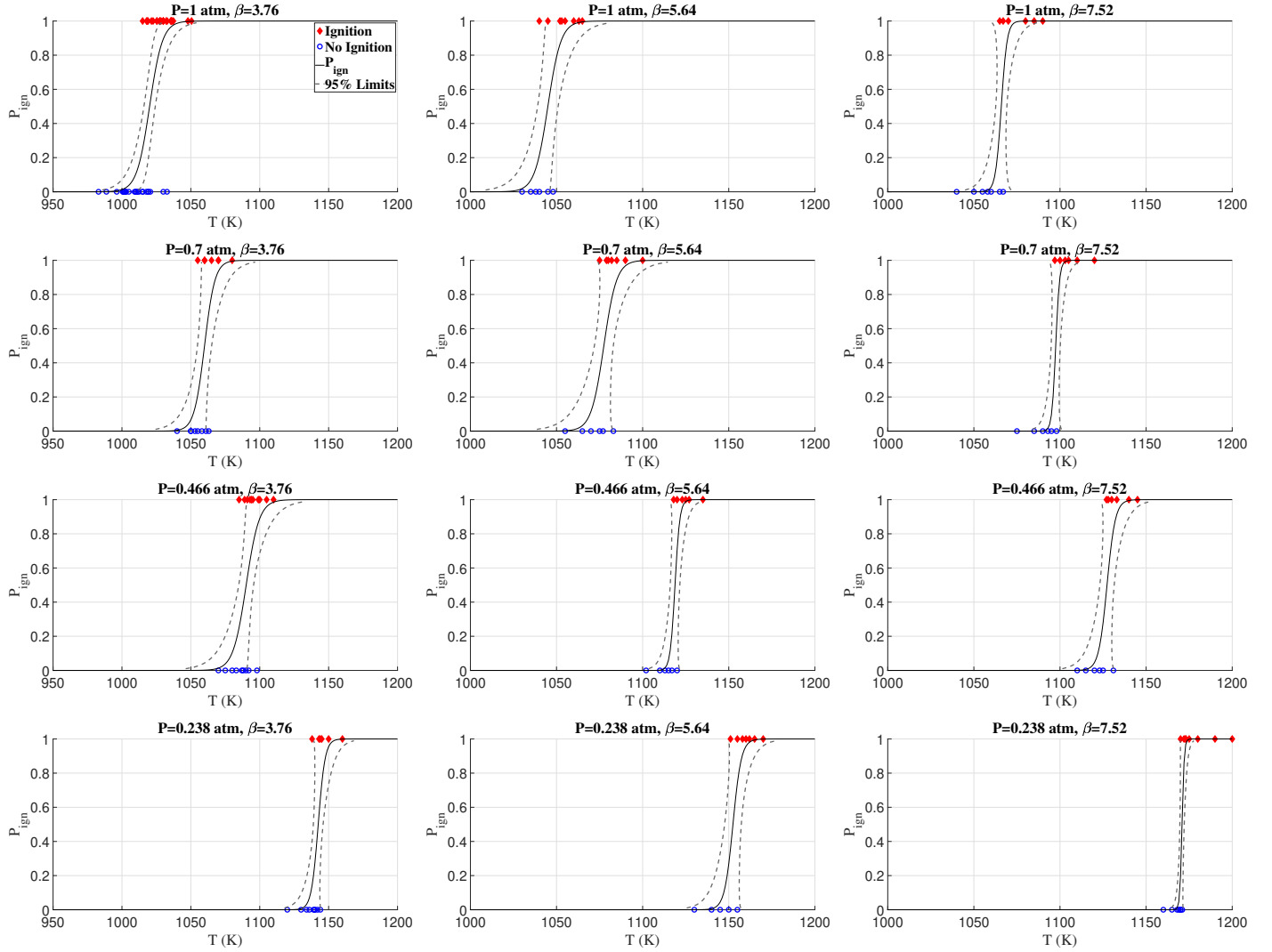


Fig. 6: Ignition data and logistic regression for hexane/air mixtures at combinations of $P_0 = 1, 0.7, 0.466, 0.238$ atm and $\beta = 3.76, 5.64, 7.52$ ($X_{O_2} = 20.6, 14.8, 11.6\%$). Pressure decreases from top to bottom and β increases from left to right.

mixtures. The magnitudes of the pressure rises can be compared to thermodynamic estimates as well as the peak pressure data from Summer (2004). For more dilute mixtures and at lower pressure, the effects of heat transfer and buoyancy on the flame are more pronounced, resulting in significant departures of the measured peak pressures from the adiabatic, constant-volume, complete-combustion (AICC) estimates as shown in Table 2. As anticipated, the AICC pressure ratios are essentially independent of initial pressure, $P_{AICC}/P_0 \approx 9.5, 8.0$ and 7.0 for $\beta = 3.76, 5.64$ and 7.52 respectively.

In contrast with Summer (2004) results, our measured peak pressures are substantially higher for even the lowest O_2 concentration (11.6%) condition and pressure (0.238 atm) tested. The peak pressure rises reported by Summer at oxygen concentrations 1-2% higher than his LOC values were on the order of 0.4 to 2.5 psi (.027 to 0.17 atm). One key difference in test procedure that may explain this is that in Summer's tests the combustion products are vented early in the ignition

Table 2: Thermodynamic estimates (AICC) and measurements of peak combustion pressure (atm) observed in the hexane testing as a function of β and initial pressure P_0 .

β	3.76	5.64	7.52	
(X _{O₂} (%))	20.6	14.8	11.6)	
P_0 (atm)				
1.0	9.58	8.08	6.95	AICC
	7.48	5.44	2.28	Experiment
0.7	6.67	5.64	4.86	AICC
	5.24	3.77	1.55	Experiment
0.466	4.41	3.74	3.23	AICC
	3.56	2.32	1.02	Experiment
0.238	2.23	1.90	1.65	AICC
	1.69	1.06	0.78	Experiment

process where our vessel remains closed throughout. The peak pressure rises in the present tests for the lowest O₂ concentration ranged from 7.3 to 17.2 psi (0.50 to 1.17 atm) for initial pressures between 0.238 and 1 atm. We also observed consistent ignition at an oxygen concentration of 11.6% at an initial pressure equivalent to 35 kft whereas Summer reported a limiting O₂ concentration of 14% at this altitude.

There are multiple factors for these differences in peak pressure and flammability limits observed in the present tests and those of Summer (2004). Our test facility used a single component gaseous fuel (hexane) with precise control over the fuel concentration rather than using the vaporization of liquid jet fuel/hexane mixtures and total hydrocarbon characterization reported by Summer. We also tested at a fixed equivalence ratio and it appears from the measurements reported by Summer that the equivalence ratio was increasing with decreasing altitude and pressure with a large variability in measured hydrocarbon concentration for tests at similar conditions. Our ignition system and mixing methods as well as the geometry of combustion vessel are significantly different than used by Summer (2004). All of these factors are known to contribute to differences in observed flammability limits.

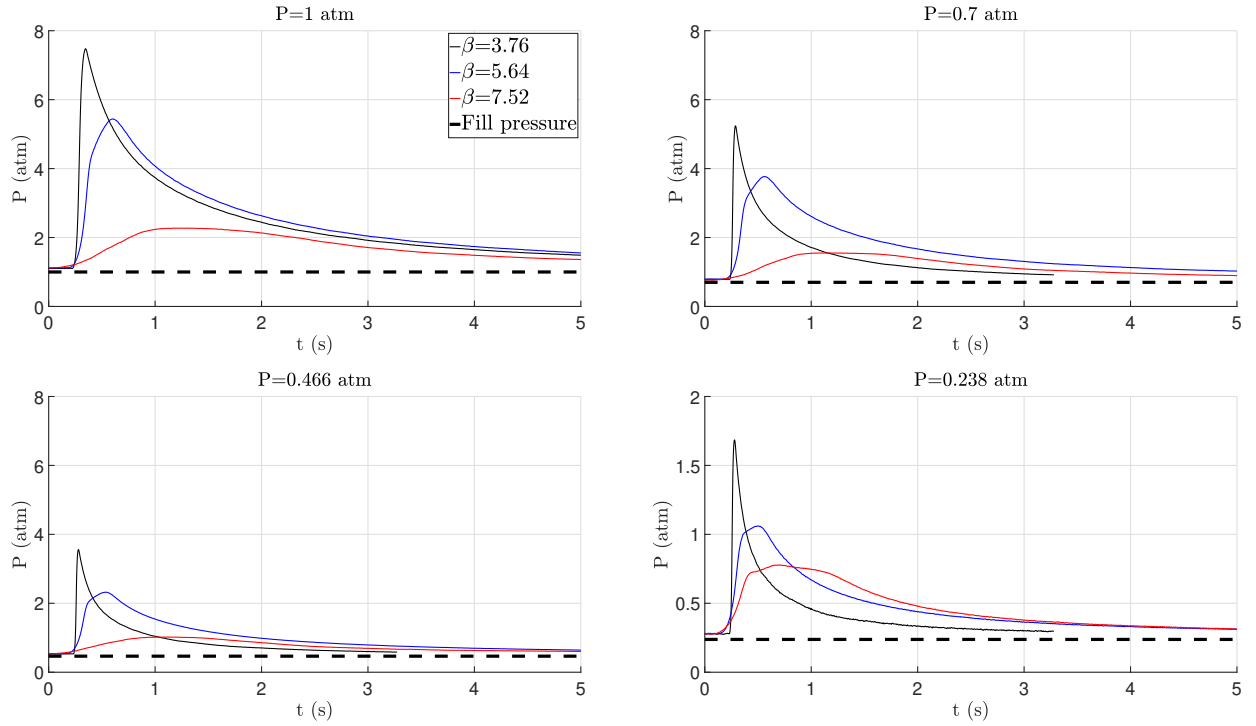


Fig. 7: Representative pressure traces from ignition in each of the sub-atmospheric *n*-hexane conditions. Note the different y-axis scaling for the $P_0 = 0.238$ atm case.

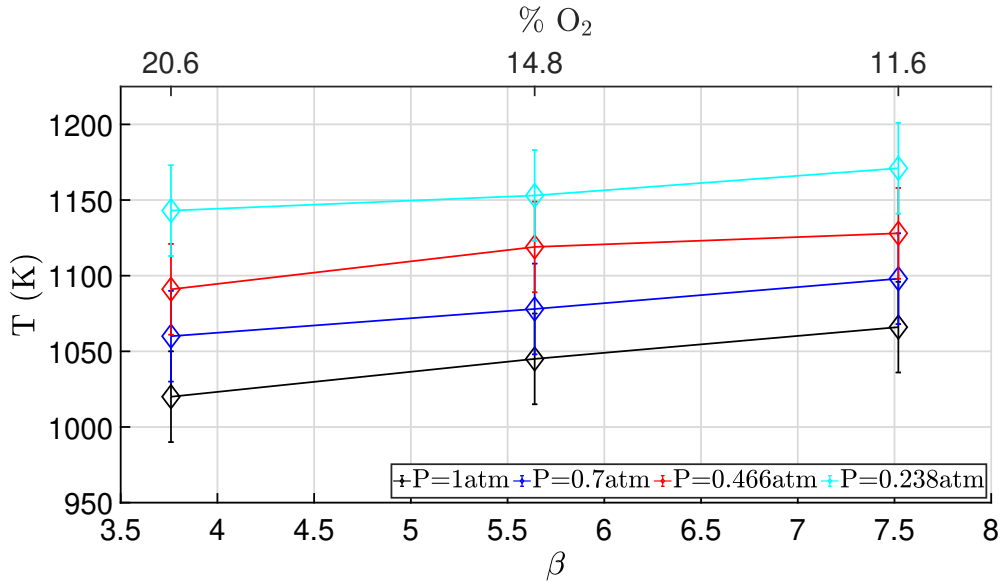


Fig. 8: Summary of ignition threshold temperatures vs β and O_2 concentration for each pressure condition.

Ono et al. (1976) proposed a semi empirical correlation for their work with a small heated flat plate. This has the form shown in equation 1 where n is a fuel-dependent constant, H is the flat plate vertical length, T_{ign} is the ignition temperature, and P_0 is the initial pressure of the flammable

mixture.

$$\ln(P_0^{n-1}H^{1/2}) = \frac{C_1}{T_{ign}} + C_2 \quad (1)$$

A least-squares fit is performed to determine the constants C_1 and C_2 using the ignition data for varying pressure at a fixed β . We note that n and H are both constant for our cases so these values are absorbed into the regression coefficients. The resulting relationship T_{ign} as a function of P_0 is shown in Fig. 9. The fit of the Ono et al. model to the present data gives confidence to the use of this model in extrapolating atmospheric pressure ignition data to lower pressures. Previous examination of this model by Jones and Shepherd (2021) demonstrated the validity of this correlation for extrapolating data obtained for a given height H over at least one order of magnitude for atmospheric hexane-air mixtures. Further work is needed and in progress in our laboratory to ground this correlation in fundamental properties of the flammable mixture in order to make this a more predictive tool.

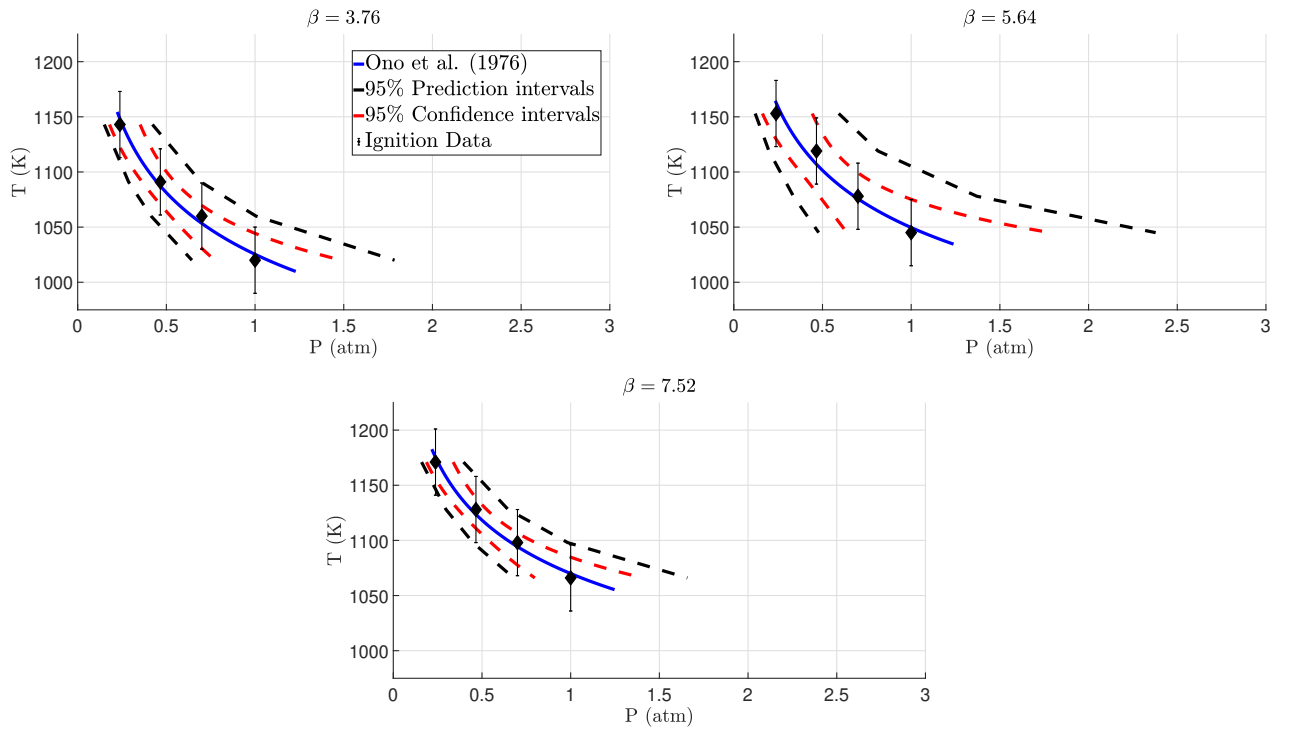


Fig. 9: Ignition temperature vs initial pressure for $\beta = 3.76, 5.64$, and 7.52 ($X_{O_2} = 20.6, 14.8, 11.6\%$). The blue line is the semi empirical correlation derived by Ono et al. (1976). The red and back dashed lines are the 95% confidence and prediction intervals computed from the linear regression.

3.4 Ignition Testing Summary

The results of the logistic regression of the ignition testing for each of the fuels is summarized in Table 3. The reported ignition temperatures are also compared with those reported from previous studies using a small cylinder and the ASTM-E659 method respectively (Boeck et al. (2017),

Martin and Shepherd (2021), Zabetakis (1965)). These results are also plotted in Figure 10 where the trend seems to be increasing ignition temperatures with fuel size in the case of external flow experiments. The opposite seems to be true for the internal flow AIT test however caution should be taken in giving any merit to the H_2 and C_2H_4 data since the AIT numbers for these are likely found using a different apparatus than the ASTM-E659.

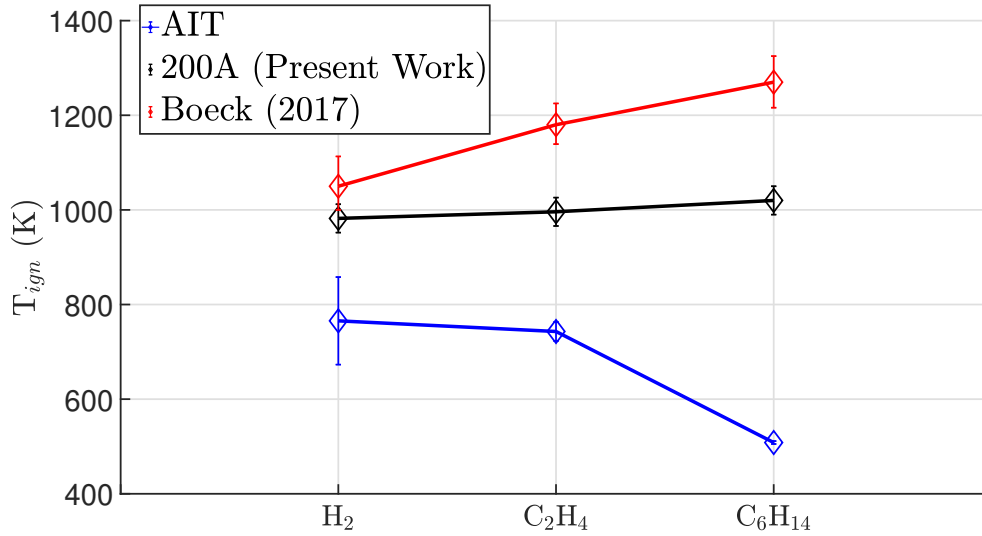


Fig. 10: Comparison of ignition temperatures for the three fuels studied with alternative ignition test methods. Error bars for H_2 and C_2H_4 ignition data represents range of values typically reported in literature.

Table 3: Ignition temperatures for all fuels as compared with previous work. Boeck et al. (2017) used a 10 mm X 10 mm cylinder. AIT values for the gaseous fuels are of uncertain provenance and the method used in obtaining these data are not always clear. ^aZabetakis (1965) ^bMartin and Shepherd (2021)

Ignition test	H_2	C_2H_4	C_6H_{14}
AIT	673 K ^a	763 K ^a	508.3 ± 3.1 K ^b
Boeck et al. (2017)	1050 K	1180 K	1270 K
Cylinder 200A (Present work)	982 ± 30 K	996 ± 30 K	1020 ± 30 K

4 Conclusions

We conclude that both decreasing pressure and increasing nitrogen dilution lead to increasing thermal ignition thresholds in hexane-air mixtures. These studies were carried out with a single type and size of ignition source, a heated vertical cylinder which produced external laminar flow. Ignition thresholds decreased approximately 100 to 150 K with a decrease in pressure from 1 to 0.238 atm. The effect of nitrogen dilution on ignition threshold at constant initial pressure was much smaller, within the range of uncertainty of the instrumentation.

In contrast to previous studies we were able to obtain ignition for oxygen concentrations as low as 11.6% for all initial pressures that we examined. The dependence of ignition temperature threshold

on initial pressure is consistent with the correlation suggested by Ono et al. (1976). Tests with hydrogen and ethylene were consistent with the trends of ignition temperature threshold dependence on fuel and the decrease in ignition temperature with increasing vertical height of the hot surface. This was consistent with the observations of Jones and Shepherd (2021) for hexane and Ono et al. (1976) for a range of fuels.

Tests with hydrogen demonstrated that surface reactions - not observed in tests with hydrocarbon fuels - had a significant effect on the wavelength dependence of thermal emission. We had to monitor the surface condition and use a cleaning regimen in order to obtain reliable surface temperature measurements using optical pyrometry.

Acknowledgements

This work was carried out in the Explosion Dynamics Laboratory of the California Institute of Technology and supported by The Boeing Company Strategic Research and Development Relationship Agreement CT-BA-GTA-1. Conor Martin was also supported by the Department of Defense (DoD) through the National Defense Science & Engineering Graduate Fellowship (NDSEG) Program.

References

- ASTM (2005). *ASTM-E659: Standard test method for autoignition temperature of liquid chemicals*.
- Bane, S. P. M., Shepherd, J. E., Kwon, E., Day, A. C. (2011). *Statistical analysis of electrostatic spark ignition of lean H₂/O₂/Ar mixtures*. International Journal of Hydrogen Energy, 36(3):2344–2350. doi:10.1016/j.ijhydene.2010.05.082.
- Boeck, L. R., Meijers, M., Kink, A., Mével, R., Shepherd, J. E. (2017). *Ignition of fuel–air mixtures from a hot circular cylinder*. Combustion and Flame, 185:265–277. doi:10.1016/j.combustflame.2017.07.007.
- Brandes, E., Hirsch, W., Stolz, T. (2017a). *Zündtemperaturen In anderen oxidationsmitteln als luft; Projekt – Zündtemperaturen brennbarer Flüssigkeiten bei erhöhtem Sauerstoffanteil im O₂+N₂-Gemisch*. Technical report, PTB Braunschweig.
- Brandes, E., Hirsch, W., Stolz, T. (2017b). *Zündtemperaturen In anderen oxidationsmitteln als luft; Projekt – Zündtemperaturen brennbarer Flüssigkeiten in Luft+N₂O-Gemisch*. Technical report, PTB Braunschweig.
- Cavage, W. M., Summer, S. (2008). *A Study of the Flammability of Commercial Transport Airplane Wing Fuel Tanks*. Final Report DOT/FAA/AR-08/8, Federal Aviation Administration, William J. Hughes Technical Center, Atlantic City International Airport, NJ.
- Coward, H. F., Jones, G. W. (1965). *Limits of Flammability of Gases and Vapors*. Technical Report BM–BULL-503, Bureau of Mines, Washington D.C. doi:10.2172/7328370.
- FAA (2017). *Operator Information for Incorporating Fuel Tank Flammability Reduction Requirements into a Maintenance and/or Inspection Program*. Advisory Circular AC No. 120-98A CHG 1, Federal Aviation Administration.
- Hirsch, W., Brandes, E. (2005). *Zündtemperaturen binärer gemische bei erhöhten ausgangsdrukken*. Technical report, PTB Braunschweig and Berlin.
- Jones, S. (2020). *Thermal Ignition by Vertical Cylinders*. Ph.D. thesis, California Institute of Technology.
- Jones, S. M., Shepherd, J. E. (2021). *Thermal Ignition by Vertical Cylinders*. Combustion and

- Flame, 232:111499. doi:10.1016/j.combustflame.2021.111499.
- Martin, C. D., Shepherd, J. E. (2021). *Low temperature autoignition of Jet A and surrogate jet fuel*. Journal of Loss Prevention in the Process Industries, 71:104454. doi:10.1016/j.jlp.2021.104454.
- Michalski, L., Michalski, L., editors (2001). *Temperature Measurement*. J. Wiley, Chichester ; New York, 2nd ed edition.
- Moravec, B. L., Boggs, R. E., Graham, R. N., Grim, A., Adkins, D. A., Snow, D., Haack, A. (2006). *Commercial Aircraft On-Board Inerting System*. US Patent No. 7,152,635 B2.
- Ono, S., Kawano, H., Niho, H., Fukuyama, G. (1976). *Ignition in a Free Convection from Vertical Hot Plate*. Bulletin of JSME, 19(132):676–683.
- Summer, S. (2004). *Limiting Oxygen Concentration Required to Inert Jet Fuel Vapors Existing at Reduced Fuel Tank Pressures-Final Phase*. Technical Report DOT/FAA/AAR-04/08, Federal Aviation Administration, William J. Hughes Technical Center, Atlantic City International Airport, NJ.
- Zabetakis, M. G. (1965). *Flammability characteristics of combustible gases and vapors*. Technical Report BM–BULL-627, 7328370, Bureau of Mines, Washington D.C. doi:10.2172/7328370.